Development of the strain visualization device and application example

Masakazu Omachi[1], Shuji Umemoto[1], Takeshi Takaki[2], Keisuke Matsuo[1], Masaki Yonemoto[1], Takashi Okada[1]

[1]Keisoku Research Consultant Co.,665-1 fukuda 1-chome higashi-ku Hiroshima-city,Japan
[2]Hhiroshima University,1-3-2 kagamiyama Higashi-hiroshima-city,Japan
email: oomachi@krcnet.co.jp, umemoto@krcnet.co.jp, takaki@hiroshima-u.ac.jp, matsuo@krcnet.co.jp,
yonemoto@krcnet.co.jp, t-okada@krcnet.co.jp

ABSTRACT: The strain visualization device is a strain measurement sensor developed to contribute to maintaining the soundness of structures.The principle of moiré fringes is used for the measurement principle of the strain visualization devicé, and the characteristic that the moiré fringes can magnify and display minute displacements makes it possible to measure minute displacements at the strain level. In addition, by simply utilizing the principle of moiré fringes, the most problematic power source for sensors for Structural Health Monitoring is not required. The strain visualization device is truly the ultimate power-saving sensor.In addition, it has unique features not found in conventional strain measurement sensors, such as (1) strain can be read directly by naked eye, (2) strain can be measured with a digital camera, (3) self-temperature compensation type, and (4) high environmental resistance performance for over 10 years.

The strain visualization device has a reading capacity of ± 500 µɛ, a visualization resolution of 50 µɛ, and a measurement accuracy of ± 10 µɛ ± 10 µɛ (2σ), which satisfies the performance as a sensor for Structural Health Monitoring.

In this paper, we show the performance and measurement method of the developed strain visualization device in detail, and also introduce the example applied to the actual structure.

KEY WORDS: Strain; Moiré; Health Monitoring; Visualization.

1 INTRODUCTION

In Japan, operation and maintenance standards for structures were strengthened following the Sasago Tunnel ceiling panel collapse accident in December 2012. Measures included enactment of legal inspection standards for bridges and tunnels and stricter periodic inspections with a frequency of once every 5 years.

Japan has approximately 720 000 bridges and 10 000 tunnels. Although operation and maintenance of this massive social capital is extremely important, at present, there is a possibility that maintenance may become impossible due to reductions in maintenance and repair budgets and the decreasing number of expert engineers engaged in maintenance work for bridges and other structures.

Because many parts of periodic inspections based on close-range visual inspection depend on manpower, and a shortage of expert engineers is foreseen in the near future, monitoring technologies that enable even unskilled personnel to determine the condition of a structure in a simple manner are strongly desired. Conventionally, structural monitoring has been performed by sensors connected to a data logger, but this method has various problems, as many structures are constructed in locations with poor accessibility, sources of electric power are not readily available, and frequent maintenance is not possible. As other problems, the cost of introduction is high, and running costs are also incurred in this method. For these reasons, monitoring has generally been limited to important, large-scale structures. However, among the above-mentioned 720 000 brides in Japan, approximately 510 000, or 71 %, are located not on national highways but on city, town, or village roads, and maintenance of these medium-

and small-scale bridges is also extremely important for protecting the lives of people.

Under such social circumstances, the authors focused on strain, which is one monitoring item, and developed a strain visualization device (Figure 1) by enabling simple, inexpensive measurement by anyone, with the aim of establishing a remote, noncontact strain measurement technique [1][2][3]. The strain visualization device is a new type of sensor for use in strain measurement which based on the principle of moiré fringes, and has the following features:

i) Strain can be visualized quantitatively.
ii) Because absolutely no electrical elements are used, a power source is not necessary and electrical malfunctions are not an issue.
iii) For the same reason, the device is not affected by electrical noise.
iv) By using an ordinary digital camera, strain can be measured remotely, without contact, and with higher accuracy than by visual inspection.
v) Maintenance is easy.

In work to date, the authors improved the measurement accuracy of the device, developed a self-temperature compensated type, and also developed an image analysis application to enable use of the strain visualization device in field measurements [1][2][3]. As described in this report, a number of improvements were made to solve several problems that arise in long-term monitoring, and practical application of the strain visualization device was successfully achieved. This paper presents details of the performance and measurement method of the developed strain visualization device and introduces an example of application to an actual structure.

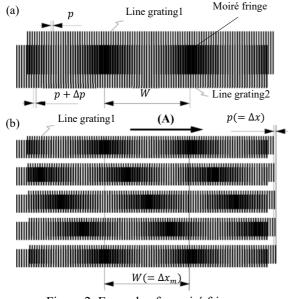Figure 1. Schematic illustration of the Strain Visualization Device

Figure 2. Example of a moiré fringe

Figure 3. Structure of Strain Visualization Device

Table 1. Specification of the strain visualization device

Gauge length	105mm
Reading capacity	±500με (F.S.=1000με)
Visualization resolution	50με
Nonlinearity	±1% of F.S.
Repeatability (2σ)	±10με
Outer dimensions	W:17×H:6.8×L:120mm

2 DEVELOPED STRAIN VISUALIZATION DEVICE

2.1 Measurement principle

As shown in Figure 2(a), when a line grating 1 with a pitch p is overlaid with a line grating 2 having a pitch $p+\Delta p$ which is Δp ($<<p$) larger than the pitch of grating 1, a striped pattern with a pitch W larger than that of gratings 1 and 2 appears. This pattern is called a moiré fringe. The strain visualization device uses the principle of moiré fringes. The relationship between the pitches of the line gratings and the pitch of the moiré fringes is expressed by Equation (1). The display of original pitch p can be visually enlarged by $(p+\Delta p)/\Delta p$ times by the moiré fringes. This magnification factor is termed M.

$$W = \frac{p+\Delta p}{\Delta p} \cdot p \qquad (1)$$

Equation (2) expresses the amount of movement Δx_m of the moiré fringes in direction A in case line grating 1 is moved Δx in direction A, as shown in Figure 2(b). In other words, the display of displacement Δx can be visually enlarged by a factor of M. This principle enables measurement of extremely small (microscopic) amounts of displacement and visualization of strain in the measurement object.

$$\Delta x_m = M \cdot \Delta x \qquad (2)$$
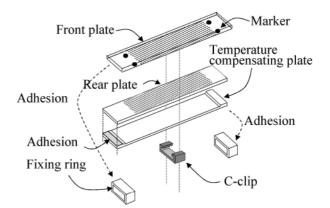
2.2 Structure and specifications

Figure 3 shows the structure of the strain visualization device. The strain visualization device comprises mainly a glass front plate and rear plate, which form the line grating or characters, and a steel temperature compensating plate, and is assembled into a unit by the fixing rings. The length, width, and thickness of the strain visualization device are 120 mm, 17 mm, and 6.8 mm, respectively, and the gauge length is 105 mm. In addition, the strain visualization device has three types of display patterns. The top row is a character pattern with a scale of 100 με pitch, which makes it possible to read strain values directly with the unaided eye, and the center row is a moiré fringe display for strain measurement by image processing. The bottom row is a fixed reference scale which is used to improve accuracy in image analysis.

Table 1 shows the specifications of the strain visualization device developed with the structure described above. Nonlinearity and repeatability were confirmed in previous laboratory tests using a precision stage [3].

2.3 Verification of performance

In long-term monitoring in outdoor environments, stable measurement for long time is required in the sensors, but the influence of temperature is frequently a problem. In addition, sensor life is sometimes reduced by deterioration caused by ultraviolet radiation, or by corrosion. Therefore, in order to verify the environmental performance of the strain visualization device, tests were conducted to verify the temperature characteristics, weathering resistance

(weatherability), and corrosion resistance of the device. The results are presented in the following sections.

(1) Temperature characteristics

When a strain visualization device is fixed to an object of measurement by gluing, and a temperature change occurs in addition to the strain caused by external force, apparent strain is generated by the difference in the linear expansion coefficients of the material being measured and the sensor used in the strain measurement. The term "self-temperature compensated strain measurement sensor" refers to a type of sensor which minimizes the apparent strain generated by temperature changes. Among strain gauges, which are a representative type of strain measurement sensor, those in which apparent strain is within ±1.8 µε/°C in the specified temperature range when affixed to a compatible material are called self-temperature compensated strain gauges. In these devices, self-temperature compensation is realized by adjusting the temperature coefficient of resistance of the resistive element of the strain gauge so as to be compatible with the material being measured.

In previous work, the authors developed strain visualization devices with a self-temperature compensate function for measurement of concrete members and steel members [2]. Figure 4 shows the relationship between the temperature of the test specimen and apparent strain. The apparent strain of the strain visualization device was less than ±1.0 µε/°C, confirming self-temperature compensation. It is particularly noteworthy that the self-temperature compensation range of the developed strain visualization device is significantly wider than that of the conventional strain gauge, as apparent strain was very small even under extreme temperature conditions, being only about 20 µε under a high temperature of 70 °C and –20 µε at –20 °C below freezing. These results demonstrated that the strain visualization device, in which a temperature compensating plate was incorporated in the device structure, is a self-temperature compensated strain measurement sensor with temperature characteristics superior to those of conventional strain gauges.

(2) Weathering resistance

An accelerated weathering test was conducted to confirm weathering resistance, that is, whether the various materials that comprise the strain visualization device are degraded by ultraviolet radiation (UV). The strain visualization device was placed in the testing device and irradiated continuously with a xenon lamp (180 W/m^2), and was also exposed to steam for 18 min during each 2 h period. The temperature in the testing device was 63 °C (38 °C during exposure to steam), and the relative humidity was 50 %.
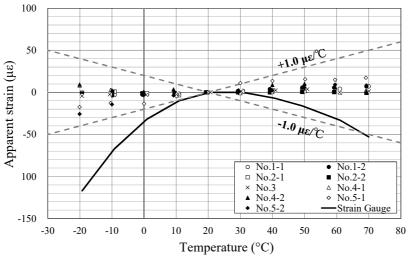

Figure 4. Relationship of specimen temperature and apparent strain

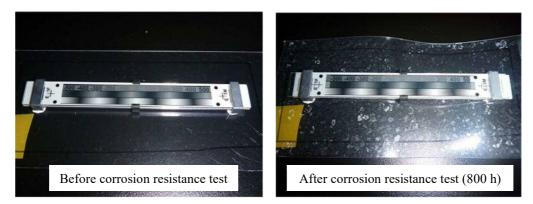| Before corrosion resistance test | After corrosion resistance test (800 h) |

Figure 5. Condition of strain visualization device before (left) and after (right) the corrosion resistance performance test

The sample was removed at specified time intervals, the strain scales were photographed, and the operation of the device was checked. The test was conducted up to a test time of about 2 000 h.

In a test conducted under the conditions described above, 200 hours of test time is equivalent to about 1 year under a natural environment.

As a result of this test, no abnormalities such as discoloration of the surface of the strain visualization device or the formed pattern were observed, and no problems were encountered in reading the strain values by visual inspection or in analysis of the photographed images during the test. Accuracy was also verified by using a precision stage after the completion of the weathering test, confirming that the device has the required performance. These tests confirmed that the weathering resistance of the strain visualization device under a natural environment is 10 years or more.

(3) Corrosion resistance

Because steel is used in some parts of the strain visualization device, the possibility that corrosion of these steel parts might affect the normal functioning of the device was a concern. Therefore, an accelerated corrosion test was carried out to confirm corrosion resistance.

The strain visualization device was placed in the testing device and subjected to a repeated cycle of saltwater spraying (5 % NaCl, 35 °C) for 2 h, drying (60 °C, 25 %RH) for 4 h, and humidity (50 °C, 98 %RH) for 2 h. The test was conducted up to approximately 800 h.

Here, 80 hours under the above-mentioned test conditions are equivalent to about 1 year under a natural environment (exposure in a coastal region).

Figure 5 shows the condition of the strain visualization device before and after the corrosion resistance test. During the test, no obvious rust was observed on the steel parts of the strain visualization device, and visual reading of the strain values and analysis of photographed images were possible without any problem. Accuracy verification using the precision stage was also performed after completion of the corrosion resistance test, and it was confirmed that the device has the required performance. These results confirmed that the strain
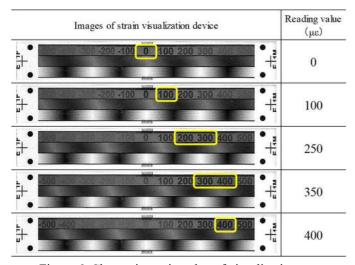
visualization device has corrosion resistance of 10 years or more under the natural environment (i.e., exposure in a coastal region).

3 MEASUREMENT METHODS

3.1 Measurement by visual inspection

Figure 6 shows an example of the change in the strain values in the visualization part (numerical characteristic display). The strain value is obtained by reading the number with the darkest appearance among numerical values with intervals of 100 με. When two numbers appear in same darkness, the strain value can be obtained with 50 με resolution by reading between those two numbers.

3.2 Measurement by digital camera

In measurement by digital camera, the camera is set up facing the strain visualization device as squarely as possible, and the device is photographed so that the black circles located in the four corners are sufficiently within the shooting screen. During photography, the photographer must be sure that the flash of the camera, the LED lighting and the background behind the photographer are not reflected on the strain visualization device.

The strain value can be calculated by analyzing the photographed image with the strain calculation application shown in Figure 7. The analysis by the strain calculation app is carried out by an import of a still image, extracting the moiré fringes, and fitting the measured values and the theoretical values of the luminance distribution of the moiré fringes. In actual operation, strain values can be calculated simply by selecting the black circles in the four corners of the strain visualization device in order and clicking the "Analyze" button.

4 EXAMPLE OF APPLICATION TO EVALUATION OF BRIDGE LOAD BEARING CAPACITY

To confirm the applicability of the strain visualization device

Figure 6. Change in strain value of visualization part

Figure 7. Stain calculation application

Figure 8. Appearance of the bridge

Table 2. Specifications of the bridge

Bridge length	102.230 m
Girder length	30.750 + 40.750 + 30.550 m
Span length	30.050 + 39.950 + 29.850 m
Effective width	Vehicle road: 6.750 m, walk way: 1.500 m
Total width	9.250 m
Superstructure construction system	Post-tensioned PC simple T-girder bridge (5 girders)
Year of construction	1975

Symbols

● : Strain visualization device   ○ : Strain gauge   △ : Deflectometer
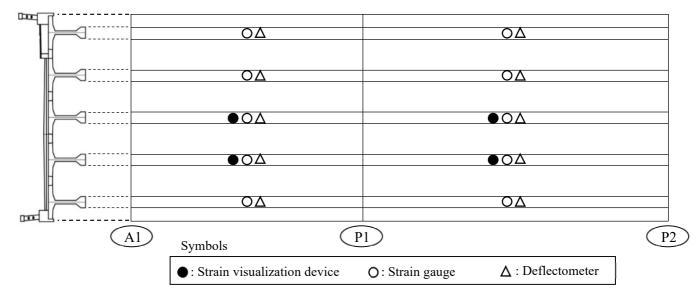
Figure 9. Arrangement of measuring devices

in the field, the device was applied to a bridge in Kagoshima Prefecture. Strain measurements were conducted during a loading test, and an evaluation of the load bearing capacity of the bridge was carried out.

4.1 Specifications of the bridge

Figure 8 and Table 2 show the appearance and specifications of the target bridge. The bridge is a 3 span post-tensioned PC simple T-girder bridge (5 girders) located in Kagoshima Prefecture.

The bridge had been in service for 46 years since construction, and a large number of cracks caused by the alkali-aggregate reaction had occurred in the main girder in the bridge axial direction.

4.2 Loading test procedure

In the evaluation of load bearing capacity, a reconstruction design is prepared based on the design standard at the time of construction and the current condition of deterioration of the bridge. Here, the validity of the reconstruction design was
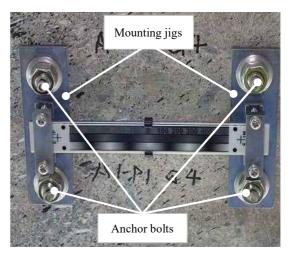

Figure 10. Condition of installation of a strain visualization device

verified by a loading test, and the load bearing capacity of the bridge against loading was confirmed.
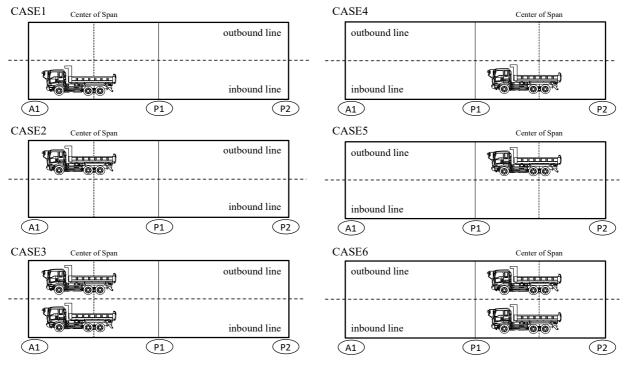
Figure 11. Loading cases

Table 3. Results of strain measurements in loading test

CASE	Strain Visualization Device （με）				Strain Gauge （με）			
	A1-P1		P1-P2		A1-P1		P1-P2	
	G3	G4	G1	G4	G3	G4	G1	G4
CASE1	24	54	-	-	32	55	-	-
CASE2	27	43	-	-	39	26	-	-
CASE3	52	64	-	-	70	81	-	-
CASE4	-	-	3	21	-	-	4	29
CASE5	-	-	8	20	-	-	27	19
CASE6	-	-	20	42	-	-	35	47

(1) Arrangement of measuring devices

Figure 9 shows the arrangement diagram of the measuring devices. The targets of verification of load bearing capacity were the A1-P1 span and the P1-P2 span. Strain gauges and deflectometers were installed on the underside of each girder in the center of the spans. Strain visualization devices were also installed near the strain gauges on girders G3 and G4 of the A1-P1 span and girders G1 and G4 on the P1-P2 span.

Figure 10 shows the condition of installation of a strain visualization device. The device was installed using dedicated mounting hardware, and was fixed to the concrete by using anchor bolts.

(2) Measurement method

The measurement method used with the strain visualization device was measurement with a digital camera, as described in the above section 3.2. First, initial images were taken in the unloaded condition, and still images were then taken for each loading case. The acquired images were analyzed by the strain calculation app shown in Figure 7, and the strain was calculated.

The measurements by the strain gauges and deflectometers were performed using dedicated instruments.

(3) Loading method

Figure 11 shows the vehicle (truck) loading cases in the loading test. The bridge was loaded with 200 kN dump truck(s) which had been weighed in advance, and the test was conducted for the case of loading on the inbound lane, the case of loading on the outbound lane, and the case of loading on both the inbound and outbound lanes on the respective spans. The bridge was loaded by dump trucks so that the center of the rear wheels of the truck was located at the center of the span in each span.

4.3 Results of loading test and evaluation of load bearing capacity

This section presents the strain measurement results for the G3 and G4 girders of the A1-P1 span and the G1 and G4 girders of the P1-P2 span, where both the strain visualization devices

and strain gauges were installed. Table 3 shows the results of the strain measurements during the loading test. The results shown for the strain visualization devices are the average value of the results of an analysis of multiple images for each loading case.

With the exception of girder G4 of the A1-P1 span for Case 2, the strain visualization devices showed slightly smaller values than the strain gauges. However, generally similar results were obtained in all cases, and the largest difference between the strain visualization device and the strain gauge was only 19 με.

This result satisfies the overall accuracy of ±20 με (nonlinearity: ±1 % of F.S., repeatability (2 σ): ±10 με), which is the specification of the strain visualization device, and verifies the applicability of the strain visualization device to field measurements.

5 CONCLUSION

The authors developed a strain visualization device that enables simple health monitoring of structures even by relatively unskilled personnel, and successfully applied the developed device under practical conditions. Laboratory tests verified that the strain visualization device has weathering resistance and corrosion resistance of 10 years or more, which is a necessary condition for long-term monitoring in the field.

Results generally in agreement with those of conventional strain gauges were obtained when the developed device was applied in an evaluation of the load bearing capacity of an actual bridge, and it was possible to confirm the validity of the reconstruction plan based on the current condition of deterioration of the bridge and the load bearing capacity of the bridge against loading. The strain visualization devices installed on the bridge will be left in place, and monitoring of time-dependent changes in strain is planned. In the future, the authors intend to accumulate actual results of long-term monitoring, and hope to contribute to health monitoring of structures.

REFERENCES

[1] Omachi, M. et al. (2015). Verification of Strain Visualization Sheet with Aim of Field Application, Proceeding of the 7th International Conference on Structural Health Monitoring of Intelligent Infrastructure, Torino,Italy, 1-3 July 2015

[2] Umemoto, S. et al. (2017). Development of Self-Temperature Compensated Strain Visualization Sheet, Proceeding of the 8th International Conference on Structural Health Monitoring of Intelligent Infrastructure, Brisbane,Australia, 5-8 December 2017

[3] Omachi, M. et al. (2017). Visualization of Strain and New Strain Measurement Technique, Proceeding of the 8th International Conference on Structural Health Monitoring of Intelligent Infrastructure, Brisbane,Australia, 5-8 December 2017